Electric Power Systems Research 114 (2014) 93–100

Contents lists available at ScienceDirect

Electric Power Systems Research

journal homepage: www.elsevier.com/locate/epsr

A linearized formulation of AC multi-year transmission expansion planning: A mixed-integer linear programming approach

Tohid Akbari*, Mohammad Tavakoli Bina

Faculty of Electrical Engineering, K.N. Toosi University of Technology, Tehran, Iran

ARTICLE INFO

Article history:
Received 21 October 2013
Received in revised form 28 March 2014
Accepted 16 April 2014

Keywords:
AC-OPF
Linearized power flow
Mixed-integer linear programming
Transmission expansion planning

ABSTRACT

This paper presents a method in expansion planning of transmission systems using the AC optimal power flow (AC-OPF). The AC-OPF provides a more accurate picture of power flow in the network compared to the DC optimal power flow (DC-OPF) that is usually considered in the literature for transmission expansion planning (TEP). While the AC-OPF-based TEP is a mixed-integer *nonlinear* programming problem, this paper transforms it into a mixed-integer *linear* programming environment. This transformation guarantees achievement of a global optimal solution by the existing algorithms and software. The proposed model has been successfully applied to a simple 3-bus power system, Garver's 6-bus test system, 24-bus IEEE reliability test system (RTS) as well as a realistic power system. Detailed case studies are presented and thoroughly analyzed. Simulations show the effectiveness of the proposed method on the TEP.

1. Introduction

Transmission expansion planning (TEP) addresses the problem of augmenting transmission lines of an existing transmission network; the objective is to optimally serve a growing electric load while satisfying a set of economical, technical and reliability constraints [1]. In general, the TEP is considered as making a stochastic decision on when (the time), where (the location), and which types of transmission lines to be installed. In [2,3], a classification scheme categorizes the subjects published in this area.

A mixed-integer linear programming (MILP) is used in [4], for the TEP problem that considers power losses. We suggest a linearization method for the AC-TEP based on the method in [4]. However, both active and reactive powers are included in our proposed formulation. In [5], a multi-year TEP model is presented using a discrete evolutionary particle swarm optimization approach. Aguado et al. [6], present a novel TEP model that considers a multi-year planning horizon in a competitive electricity market. Both the TEP and generation expansion planning (GEP) problems are analyzed together in [7,8]. Also, transmission switching (TS) is investigated in [9] for the TEP showing that the TS could improve the capacity expansion planning model as well as reducing the total planning cost. A meta-heuristic and holistic approach is presented in [10] for the TEP which has been tested on a realistic power system. In [11], a scenario-based multi-objective model is presented for multi-stage TEP where the non-dominated sorting genetic algorithm (NSGA-II) is used to overcome the difficulties in solving the non-convex mixed-integer optimization problem. A multi-objective framework is presented in [12] for the TEP in deregulated environment. Recently, intermittent energy resources have been experiencing a rapid growth in power generation around the world. Therefore, new challenges are introduced to integrate the renewable energy sources (RES) to the power grid. There are many published papers which focus on this newly main issue [13–15].

The planner of power system should deal with many uncertainties during the planning process such as load uncertainty, uncertainty in prices, market rules and etc. A multistage TEP problem including available transfer capability (ATC) is modeled in [16] that takes load uncertainty into account by considering several scenarios generated by Monte Carlo simulation. In [17], the TEP is studied by considering the load uncertainty using benders decomposition. Since this paper is focused on transforming a mixed-integer nonlinear programming (MINLP) problem into a MILP, uncertainties have not been considered in this paper. However, the presented model can easily be extended for taking uncertainties into account.

The surveyed literatures use the DC-OPF for solving the TEP problem which is not completely suitable due to ignoring reactive power. However, there have been some published papers which use the AC-OPF to solve the TEP problem [18–21]. This paper proposes an approach for transmission planning based on the AC-OPF,

* Corresponding author. Tel.: +98 0912 5179374; fax: +98 21 88462066.
E-mail addresses: tohidakbari@yahoo.com, tohidakbari@ee.kntu.ac.ir (T. Akbari).

http://dx.doi.org/10.1016/j.epsr.2014.04.013
0378-7796/

Nomenclature

Indices

g	index of generators
i, j	indices of buses
l	index of lines
m	index of blocks used for piecewise linearization
t	index of sub-periods (times)

Sets

B	set of all buses
CL	set of all candidate lines
CL_i	set of all candidate lines connected to bus i
EL	set of all existing lines
EL_i	set of all existing lines connected to bus i
G	set of all generators
SP	set of all sub-periods

Constants

$AP_{L.l}^{\max}$	maximum apparent power flow of line l
I	interest rate
IC_l	investment cost of candidate line l
M	number of blocks used for piecewise linearization
nc	number of candidate lines
ng	number of generators
$P_{D,it}$	active power demand at bus i in time t
$Q_{D,it}$	reactive power demand at bus i in time t
$P_{G,g}^{\min}$	minimum active power of generator g
$P_{G,g}^{\max}$	maximum active power of generator g
$Q_{G,g}^{\min}$	minimum reactive power of generator g
$Q_{G,g}^{\max}$	maximum reactive power of generator g
$\lvert V_i^{\min}\rvert$	minimum of the voltage magnitude at bus i
$\lvert V_i^{\max}\rvert$	maximum of the voltage magnitude at bus i
Y_{ij}^0, Y_{ij}	admittance of line ij for the existing and candidate lines, respectively. ($Y_{ij}^0 = G_{ij}^0 + jB_{ij}^0$, $Y_{ij} = G_{ij} + jB_{ij}$)
$\alpha_{ij,m}$	slope of the mth block of the voltage angle difference between corridor i and j
$\Delta\theta_{ij}$	maximum of each block width for corridor i and j
θ_{ref}	voltage phase angle for the slack bus ($\theta_{ref} = 0$)
σ	a constant to make investment and operation cost comparable
$\tau_{ij}, \upsilon, \omega_{ij}, \psi_1, \xi_{ij}$,	disjunctive parameters

Variables:

IC_t	investment cost in time t
OC_t	operation cost in time t
OF	objective function
$P_{G,gt}$	active power of generator g in time t
$P_{L_{i\to j},lt}^0$	active power flow of existing line l from bus i to bus j in time t
$P_{L_{i\to j}}, lt$	active power flow of candidate line l from bus i to bus j in time t
$Q_{G,gt}$	reactive power of generator g in time t
$Q_{L_{i\to j},lt}^0$	reactive power flow of existing line l from bus i to bus j in time t
$Q_{L_{i\to j}}, lt$	reactive power flow of candidate line l from bus i to bus j in time t
u_{lt}	binary variable related to the candidate lines in time t
$\lvert V_{it}\rvert$	voltage magnitude at bus i in time t
$\theta_{ij,mt}$	width of the mth angle block of corridor i and j in time t
$\theta_{ijt}^+, \theta_{ijt}^-$	positive variables used so as to eliminate the absolute function
θ_{it}	voltage angle at bus i in time t

providing a more accurate picture of both active and reactive power flows in the expanded power network in the future planning horizon. The novelty of this paper is the introduction of a MILP formulation using the AC-OPF approach so as to solve the expansion planning problem of transmission grid. In brief, an AC-OPF-based TEP is formulated, and linearized around the operating point in order to derive a MILP problem. Solving a MILP problem is a mature technology, where the MILP solvers can be embedded in many tools and applications. Moreover, some numerical examples are presented in which simulations are discussed accordingly. The whole linearization process provided in subsection "B" of section "II" that converts the non-linear AC approach to a MIP problem is novel and has not been previously presented. This paper contributes to the TEP by approximating the sine and cosine functions in power flow equations by their Taylor's series; then, the quadratic function is modeled using piecewise linear functions. Moreover, the inequality constraints for apparent powers of existing and candidate lines are transformed into a set of linear constraints. Numerical results confirm the contribution of the proposed method in comparison with the conventional solutions. Since the proposed optimization problem for solving the TEP is linear, the global optimal solution can be obtained easily by the available software. In addition, outcomes obtained by the proposed method are more accurate (due to taking reactive power into account) than those of the available conventional methods (due to ignoring reactive power by using the DC-OPF for solving the TEP). It should be emphasized that the ISO (independent system operator) is responsible for transmission expansion planning; the ISO aims at minimizing the investment cost plus the total payment to the generating companies.

2. Analysis and formulation of the TEP

Here the proposed method is formulated, presenting the TEP based on the AC-OPF using a MINLP that will be transformed into a MILP.

2.1. The AC-OPF-based TEP formulation

The objective function is the investment cost (IC) which is the construction cost of new lines and transformers (if any) plus the operation cost (OC). The OC includes the total cost of generation in the power system under study. Using an AC power flow, objective function of the TEP can be formulated as follows:

$$\text{Min } OF = \sum_{t\in SP}(1+I)^{-t}\left(\underbrace{\sum_{l=1}^{nc} u_{lt}IC_l}_{\text{Investment cost in time } t(IC_t)} + \sigma \underbrace{\sum_{g=1}^{ng} C_g P_{G,gt}}_{\text{Operation cost in time } t(OC_t)}\right) \quad (1)$$

The objective function (1) is subjected to the following equality and inequality constraints;

Equality constraints:

$$P_{G,it} - P_{D,it} = \sum\nolimits_{l\in EL_i} P_{L_{i\to j},lt}^0 + \sum\nolimits_{l\in CL_i} P_{L_{i\to j},lt} \quad \forall i, j \in B, \forall t \in SP \quad (2)$$

$$Q_{G,it} - Q_{D,it} = \sum\nolimits_{l\in EL_i} Q^0_{L_{i\to j},lt} + \sum\nolimits_{l\in CL_i} Q_{L_{i\to j},lt} \quad \forall i,j\in B, \forall t\in SP \tag{3}$$

$$P^0_{L_{i\to j},lt} = |V_{it}|^2 G^0_{ij} - |V_{it}||V_{jt}| \times (G^0_{ij}\cos(\theta_{it}-\theta_{jt}) + B^0_{ij}\sin(\theta_{it}-\theta_{jt})) \quad \forall i,j\in B, \forall l\in EL, \forall t\in SP \tag{4}$$

$$P_{L_{i\to j},lt} = u_{lt}(|V_{it}|^2 G_{ij} - |V_{it}||V_{jt}| \times (G_{ij}\cos(\theta_{it}-\theta_{jt}) + B_{ij}\sin(\theta_{it}-\theta_{jt}))) \quad \forall i,j\in B, \forall l\in CL, \forall t\in SP \tag{5}$$

$$Q^0_{L_{i\to j},lt} = |V_{it}|^2 B^0_{ij} - |V_{it}||V_{jt}| \times (G^0_{ij}\sin(\theta_{it}-\theta_{jt}) + B^0_{ij}\cos(\theta_{it}-\theta_{jt})) \quad \forall i,j\in B, \forall l\in EL, \forall t\in SP \tag{6}$$

$$Q_{L_{i\to j},lt} = u_{lt}(|V_{it}|^2 B_{ij} - |V_{it}||V_{jt}| \times (G_{ij}\sin(\theta_{it}-\theta_{jt}) + B_{ij}\cos(\theta_{it}-\theta_{jt}))) \quad \forall i,j\in B, \forall l\in CL, \forall t\in SP \tag{7}$$

Inequality constraints:

$$P^{\min}_{G,g} \le P_{G,gt} \le P^{\max}_{G,g} \quad \forall g\in G, \forall t\in SP \tag{8}$$

$$Q^{\min}_{G,g} \le Q_{G,gt} \le Q^{\max}_{G,g} \quad \forall g\in G, \forall t\in SP \tag{9}$$

$$(P^0_{L_{i\to j},lt})^2 + (Q^0_{L_{i\to j},lt})^2 \le (AP^{\max}_{L,l})^2 \quad \forall l\in EL, \forall t\in SP \tag{10}$$

$$(P_{L_{i\to j},lt})^2 + (Q_{L_{i\to j},lt})^2 \le u_{lt}(AP^{\max}_{L,l})^2 \quad \forall l\in CL, \forall t\in SP \tag{11}$$

$$|V^{\min}_i| \le |V_{it}| \le |V^{\max}_i| \quad \forall i\in B, \forall t\in SP \tag{12}$$

$$u_{1(t+1)} \ge u_{1t} \quad \forall l\in CL, \forall t\in SP \tag{13}$$

While (1) shows the objective function, i.e. *IC* plus *OC*, (2) and (3) represent active and reactive power balance at each bus, respectively. Constraints (4) and (5) indicate active power flowing through existing and candidate lines, respectively. Similarly, constraints (6) and (7) introduce reactive power flows through existing and candidate lines, respectively. Superscript index 0 is used to denote the existing lines. Active and reactive power generation limits of the generators are represented by (8) and (9). Transmission power limits are shown by (10) and (11) for both the existing and candidate lines, respectively. Voltage magnitude limits are shown by (12). Eq. (13) implies that if a candidate line is constructed within the sub-period t, it is considered as an existing line in the next sub-period.

The above-formulated problem is a MINLP problem due to the nonlinearities in (4)–(7) as well as in (10)–(11). It should be noted that the obtained solution for the model (1)–(12) is a practical feasible local optimum solution that meets the requirements of ISO; but, not a global one. This is due to the non-convexity nature of the formulated problem. However, when one tries solving a non-convex MINLP optimization problem, there will be no guarantee to obtain the global optimum solution. This restriction remains unresolved for the most practical optimization models in a complex system [22,23].

Hence, the proposed MINLP problem is transformed into an MILP to avoid any local optimal solutions. This obtained MILP formulation is an approximate for the original AC formulation. Further, the global optimal solution of the MILP formulation can efficaciously be obtained by existing solvers. While the resultant solution is *not* necessarily the same as the global optimal solution of the MINLP formulation (hardly attainable and no guarantee to reach it), the MILP solution remains close to the global solution of original MINLP problem depending on the number of blocks in modeling the circle or quadratic terms (M or n).

2.2. Linearization of the presented MINLP

Here it is introduced the linearization of the MINLP, presented by (1)–(12), around the normal operating point. Let us assume the phase difference between the voltages at both ends of every existing or constructed lines is small enough; this implies validation of first order approximation of sine and cosine functions in their Taylor series. Moreover, assume the voltage magnitudes are nearly 1 p.u. for all buses. These assumptions are practically true under normal operating condition, maintaining the system far from instability and other security limits. Based on the aforementioned assumptions, (4)–(7) can be re-arranged by substituting sine and cosine functions in their Taylor series expansion about zero. In the following formulation, just for the sake of simplicity, we have dropped the subscript t. It can be added to the corresponding variables or parameters if referring to sub-period t.

$$P^0_{L_{i\to j},l} = G^0_{ij}(1-\cos(\theta_i-\theta_j)) - B^0_{ij}\sin(\theta_i-\theta_j) \cong G^0_{ij}\left(\frac{(\theta_i-\theta_j)^2}{2}\right) - B^0_{ij}(\theta_i-\theta_j) \quad \forall i,j\in B, \forall l\in EL \tag{14}$$

$$P_{L_{i\to j},lt} = u_1(G_{ij}(1-\cos(\theta_i-\theta_j)) - B_{ij}\sin(\theta_i-\theta_j)) \cong u_1\left(G_{ij}\left(\frac{(\theta_i-\theta_j)^2}{2}\right) - B_{ij}(\theta_i-\theta_j)\right) \quad \forall i,j\in B, \forall l\in EL \tag{15}$$

$$Q^0_{L_{i\to j},lt} = -B^0_{ij}(1-\cos(\theta_i-\theta_j)) - G^0_{ij}\sin(\theta_i-\theta_j) \cong -B^0_{ij}\left(\frac{(\theta_i-\theta_j)^2}{2}\right) - G^0_{ij}(\theta_i-\theta_j) \quad \forall i,j\in B, \forall l\in EL \tag{16}$$

$$Q_{L_{i\to j},l} = u_1(-B_{ij}(1-\cos(\theta_i-\theta_j)) - G_{ij}\sin(\theta_i-\theta_j)) \cong u_1\left(-B_{ij}\left(\frac{(\theta_i-\theta_j)}{2}\right)^2 - G_{ij}(\theta_i-\theta_j)\right) \quad \forall i,j\in B, \forall l\in CL \tag{17}$$

Then, the second order functions in (14)–(17) can be linearized by considering $2M$ piecewise linear blocks as shown in Fig. 1, approximating the existing line l between corridors i and j as below:

$$(\theta_i-\theta_j)^2 = \sum_{m=1}^{M}\alpha_{ij,m}\theta^0_{ij,m}, \quad \forall i,j\in B \tag{18}$$

$$|\theta_i-\theta_j| = \sum_{m=1}^{M}\theta^0_{ij,M}, \quad \forall i,j\in B \tag{19}$$

$$0 \le \theta^0_{ij,m} \le \Delta\theta_{ij}, \quad \forall i,j\in B \tag{20}$$

$$\alpha_{ij,m} = (2m-1)\Delta\theta_{ij} \quad m=1,\ldots,M\ \forall i,j\in B \tag{21}$$

where $\alpha_{ij,m}$ and $\theta^0_{ij,m}$ are the slope and the value of the mth block of phase difference between corridors i and j, respectively. The slope can be calculated according to (21). The same constraints will be applied to the candidate lines. However, (20) should be rewritten for candidate lines as follow:

$$0 \le \theta_{ij,m} \le \Delta\theta_{ij} + (1-u_1)\xi_{ij} \quad \forall i,j\in B \tag{22}$$

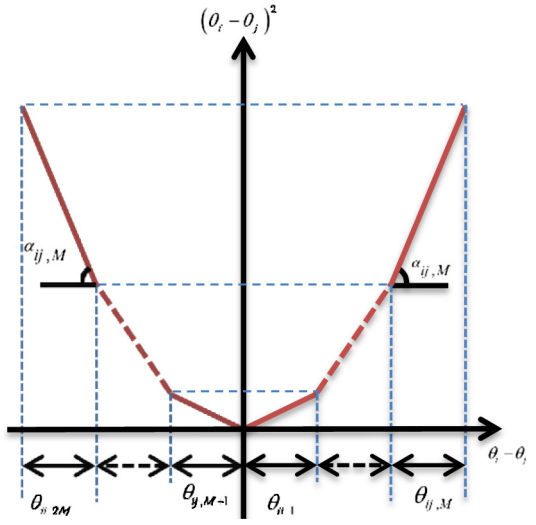

Fig. 1. Piecewise linear modeling of loss function.

The disjunctive parameter ξ_{ij} should be large enough to avoid restriction of the width of the mth phase difference between the two nodes i and j. In (22), if a candidate line l is constructed, the block width will be bounded above by $\Delta\theta_{ij}$; otherwise, for a sufficient big number ξ_{ij}, the above constraint will be nonbinding. An appropriate value for $\Delta\theta_{ij}$ can be 2π.

The nonlinearity in (19) (the absolute function) can be eliminated by introducing two extra positive variables θ_{ij}^{+} and θ_{ij}^{-} as follows:

$$|\theta_i-\theta_j|=\theta_{ij}^{+}+\theta_{ij}^{-} \quad \forall i,j\in B \tag{23}$$

$$\theta_i-\theta_j=\theta_{ij}^{+}-\theta_{ij}^{-} \quad \forall i,j\in B \tag{24}$$

$$\theta_{ij}^{+}\geq 0 \text{ and } \theta_{ij}^{-}\geq 0, \quad \forall i,j\in B \tag{25}$$

Applying the above linearization method to (14)–(17) will remove the nonlinearities in both (14) and (16). However, the nonlinearities in (15) and (17) will still remain in place due to the product of discrete and continuous variables (u_1 by θ_i). These nonlinearities can be eliminated by introducing constant large enough numbers ω_{ij} and τ_{ij} as follows:

$$-(1-u_1)\omega_{ij}\leq P_{L_{i\to j},l}+B_{ij}\times(\theta_i-\theta_j)-G_{ij}\frac{\sum_{m=1}^{M}\alpha_{ij,m}\theta i_{j,m}}{2}\leq(1-u_1)\omega_{ij}, \quad \forall i,j\in B,\ \forall l\in CL \tag{26}$$

$$-(1-u_1)\tau_{ij}\leq Q_{L_{i\to j},l}+G_{ij}\times(\theta_i-\theta_j)-B_{ij}\frac{\sum_{m=1}^{M}\alpha_{ij,m}\theta i_{j,m}}{2}\leq(1-u_1)\tau_{ij}, \quad \forall i,j\in B,\ \forall l\in CL \tag{27}$$

Appropriate values for ω_{ij} and τ_{ij} can be selected as below:

$$\omega_{ij}=2\pi^2G_{ij}-2\pi B_{ij} \tag{28}$$

$$\tau_{ij}=2\pi G_{ij}-2\pi^2B_{ij} \tag{29}$$

It should be emphasized that the above linearization technique adds three sets of continuous variables to the problem, $\theta_{ij,m}^{0}(\theta_{ij,m})$, θ_{ij}^{+} and θ_{ij}^{-} ($M+2$ variables for each line between corridors i and j). Further, nonlinearity in (10) can be removed by introducing the following n equations (see Appendix for more details and explanations):

$$\left(\sin\left(\frac{360^\circ k}{n}\right)-\sin\left(\frac{360^\circ}{n}(k-1)\right)\right)P_{L_{i\to j},l}^{0}-\left(\cos\left(\frac{360^\circ k}{n}\right)-\cos\left(\frac{360^\circ}{n}(k-1)\right)\right)Q_{L_{i\to j},l}^{0}-AP_{L,l}^{\max}\times\sin\left(\frac{360^\circ}{n}\right)\leq 0 \quad k=1,\ldots,n,\ \forall l\in EL \tag{30}$$

The corresponding equation for candidate lines can also be like:

$$u_1\left(\sin\left(\frac{360^\circ k}{n}\right)-\sin\left(\frac{360^\circ}{n}(k-1)\right)\right)P_{L_{i\to j},l}-\left(\cos\left(\frac{360^\circ k}{n}\right)-\cos\left(\frac{360^\circ}{n}(k-1)\right)\right)Q_{L_{i\to j},l}-AP_{L,l}^{\max}\times\sin\left(\frac{360^\circ}{n}\right)\leq 0, \quad k=1,\ldots,n,\ \forall l\in CL \tag{31}$$

It can be seen that (31) is still nonlinear due to the multiplication of discrete and continuous variables (product of u_1 by $P_{L_{i\to j}}l$ and $Q_{L_{i\to j}}l$). In order to make (31) linear, a second step should be taken further by using the following three relationships:

$$-u_1\times\psi_1\leq P_{L_{i\to j}}\leq u_1\times\psi_1, \quad \forall l\in CL \tag{32}$$

$$-u_1\times\psi_1\leq Q_{L_{i\to j},l}\leq u_1\times\psi_1, \quad \forall l\in CL \tag{33}$$

$$\left(\sin\left(\frac{360^\circ k}{n}\right)-\sin\left(\frac{360^\circ}{n}(k-1)\right)\right)P_{L_{i\to j},l}-\left(\cos\left(\frac{360^\circ k}{n}\right)-\cos\left(\frac{360^\circ}{n}(k-1)\right)\right)Q_{L_{i\to j},l}-AP_{L,l}^{\max}\times\sin\left(\frac{360^\circ}{n}\right)\leq 0 \quad k=1,\ldots,n,\ \forall l\in CL \tag{34}$$

A suitable amount for ψ_1 can be the maximum apparent power for line l, i.e. $AP_{L,l}^{\max}$. If candidate line l is selected, (34) restricts active and reactive power flow such that constraints (32) and (33) will be nonbinding. Otherwise, constraints (32) and (33) will limit active and reactive powers to zero so that (34) will be nonbinding. Note that $\sin(360^\circ/n)$ is always positive ($n\geq 4$). Thus, linearization of (10) and (11) requires using n linear equations for each existing line along with $n+2$ equations for each candidate line instead of using one equation. Therefore, as the number n becomes larger, the search space gets larger as well. As a solution for this case, first the method can be applied to the high-voltage transmission lines in order to reduce the search space; second, the planning can be conducted for lower voltage level transmission lines.

3. Numerical example

The proposed model has been successfully applied to four different power systems; a simple 3-bus power system, Garver's 6-bus test system, IEEE 24-bus reliability test systems (RTS) and Iranian 400-kV network. This problem was solved on a PC running with Core 2 Duo CPU, clocking at 2.00 GHz and 1 GB RAM. The used software is CPLEX 12.2.0.2 under GAMS 23.6.3 (General Algebraic Modeling System) [24]. Cplex is a commonly used solver to solve the MIP problems which can efficaciously get to the global optimal solution. This solver uses the branch and cut algorithm.

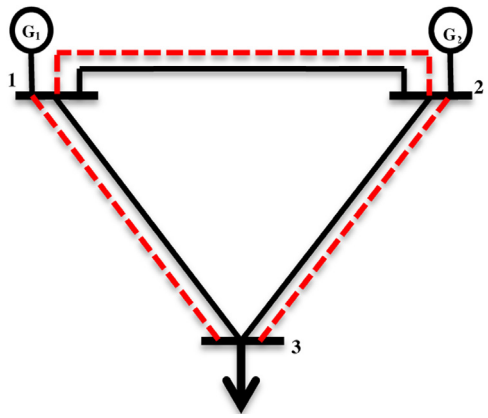

Fig. 2. A simple 3-bus test system.

3.1. First case study: a simple 3-bus test system

First, a very simple 3-bus power system is assumed to show the effectiveness of the method as shown in Fig. 2. The capacity of all existing and candidate transmission lines is supposed to be 220 MVA. Admittance of all existing and candidate lines is assumed to be $Y_{ij}^0 = Y_{ij} = 15 + j(-60)$ Investment cost of candidate lines 1, 2 and 3 are 7×10^6, 8×10^6 and 9×10^6, respectively. Offer coefficients of generators 1 and 2 are equal to 20 $/MWh which are located at buses 1 and 2, respectively. Demand at bus 3 is considered to be $P_D + jQ_D = 600 + j100$. The maximum active and reactive power of generators are 320 MW and 64 MVAr.

Here it is compared the simulations for the DC-TEP, the AC-TEP and the linearized AC-TEP (LAC-TEP) approach. For the sake of simplicity, the objective function is assumed to be the investment cost of lines, excluding the operation cost of generators. In the AC-based approach, the voltage magnitudes of buses are limited to 0.95 and 1.05 p.u. For the AC-TEP, the objective function (OF) will be 1.7×10^7 and candidate lines 2 and 3 are selected as the optimal solution. The active power generation of units 1 and 2 are 320 MW and 283.4 MW, respectively. For the LAC-TEP method, the OF is the same as that of the AC-TEP and active power generation of units 1 and 2 are 320 MW and 293.5 MW, respectively. However, the results for the DC-TEP are different from those of both the AC-TEP and the LAC-TEP; the OF is 1.5×10^7 and candidate lines 1 and 2 is selected as optimal solution. Units 1 and 2 generate 320 MW and 280 MW, respectively. Table 1 compares the simulations for all the three methods.

3.2. Second case study: Garver's 6-bus test system

The Garver test system is depicted in Fig. 3 [4]. It has six buses, 15 candidate branches, and a total demand of 760 MW. Generators, loads and lines data can be found in [4]. Reactive power demand is assumed to be 20% of active power demand for each bus. Maximum

Table 1
Simulation data for the 3-bus test system.

Statistic data	Method		
	DC-TEP	AC-TEP	LAC-TEP
Number of blocks of equations	11	15	26
Number of blocks of variables	6	10	14
Number of non-zero elements	325	346	4087
Number of single equations	143	129	1788
Number of single variables	45	86	464
Number of discrete variables	3	3	3
Execution time (s)	0.015	0.016	0.187

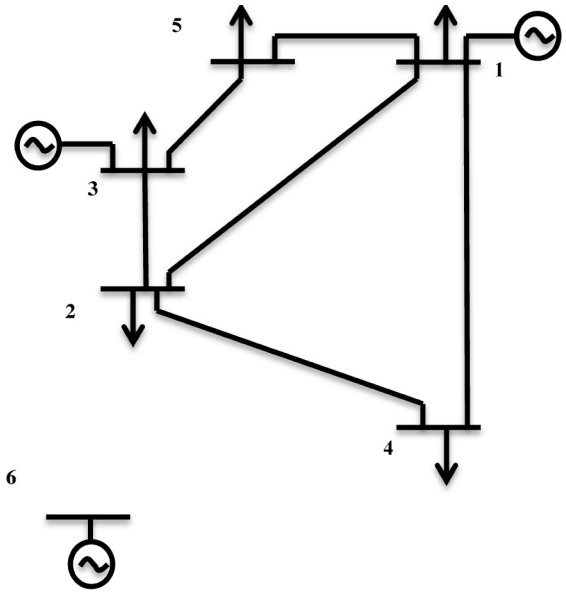

Fig. 3. Garver's 6-bus test system.

reactive power for each generator is assumed to be one third and one fifth of its generated maximum active power under lagging and leading operating conditions, respectively.

First, it is assumed that $n = 16$ for the LAC-TEP (i.e. a 16-sided convex regular polygon is considered to model the circle as described in Appendix) and $\sigma = 0$ (i.e. the objective function takes no operating cost into account). The execution time was 0.234 s. Table 2 shows simulation data reported by the GAMS. The value of objective function, i.e. the investment cost, is $\$5.14 \times 10^8$. Simulation results show lines 1, 2, 3, 5, 6, 7, 9, 10, 11, 12, 14 and 15 should be built within the planning horizon. Generators 1, 2 and 3 will produce 150 MW, 360 MW and 291 MW together with 7.6 MVAr, −24.0 MVAr and −29.2 MVAr, respectively. This means the total power losses for the system is about 41 MW or 5.12% of the total active power generations.

Second, the number of sides of the regular polygon was set to be equal to 8. The problem will become integer infeasible in this case. This occurs because when the number of sides of the regular polygon (n) becomes smaller, transmission of both active and reactive powers become more limited through the lines. Thus, the number of sides was set to be equal to 32 ($n = 32$), resulting in $\$4.36 \times 10^8$ for the objective function and candidate lines to be built were 3, 5, 6, 7, 9, 10, 11, 12, 14 and 15. This shows that some transmission

Table 2
Simulation data for the Garver's 6-bus system.

Number of blocks of equations	26	Number of single equations	19,483
Number of blocks of variables	14	Number of single variables	7018
Number of non-zero elements	41,872	Number of discrete variables	15

Table 3
LMP of buses of Garver's 6-bus system.

Bus	LMP ($/MWh)
1	33.3
2	34.4
3	30.8
4	34.9
5	34.4
6	30.0

Table 4
Candidate lines data.

Candidate lines			Capacity (MVA)	Reactance (p.u.)	Investment cost (10^6US)
Name	From	To			
CL_1	1	4	175	0.015	7.72
CL_2	2	7	175	0.021	10.82
CL_3	7	10	175	0.020	10.29
CL_4	9	10	175	0.016	8.24
CL_5	11	15	500	0.022	11.13
CL_6	11	20	500	0.024	12.35
CL_7	11	24	500	0.011	5.66
CL_8	13	20	500	0.011	5.66
CL_9	14	19	500	0.017	8.76
CL_{10}	19	21	500	0.014	7.21
CL_{11}	20	22	500	0.014	7.21

Table 5
Results for different value of σ.

σ (h)	IC ($)	Candidate lines to be built	OC ($/h)	OF ($)
5×8760	7.21×10^6	CL10	123,892.876	6.1475×10^7
15×8760	1.442×10^7	CL10, CL11	118,128.524	1.6964×10^8
25×8760	2.008×10^7	CL8, CL10, CL11	113,884.071	2.6949×10^8

lines are operating at their capacity limits. The number of non-zero elements and single equations are 60,304 and 28,699, respectively. Other simulation data for the AC-OPF and the DC-OPF are the same as those of listed in Table 2. Execution time reported by the GAMS was about 0.296 s.

Third, for $n = 64$ in the LAC-OPF, the objective function will become $\$4.34 \times 10^8$ and candidate lines to be built were 2, 3, 5, 6, 9, 10, 11, 12, 14 and 15. For $n > 64$, simulations remain unchanged. Therefore, one should be careful in determining the number of segments used to model the circle. Using the AC-TEP will result in the construction of the same lines as those of the LAC-TEP under $n = 64$ with the exception of building line 13 instead of line 12; the objective function for the AC-OPF becomes $\$5.29 \times 10^8$ that is bigger than that of the LAC-OPF.

Assuming $\sigma = 10 \times 8760$,[1] the *IC* and *OC* are equal to $\$4.34 \times 10^8$ and $17,398.7 per hour for $n = 64$. This means the same candidate lines are constructed when considering operation cost. The Lagrangian multiplier of active power balance equation or locational marginal price (LMP) for bus numbers 1–6 are listed in Table 3.[2] It should be highlighted that these LMPs are obtained after fixing the binary variables of candidate lines to their corresponding optimal values of the optimization problem. Note that the generator connected across bus 6 is the marginal generator. Table 3 shows LMPs are different at those buses since power losses are not ignored. It should also be noted that there is no congestion in transmission lines.

3.3. Third case study: the IEEE 24-bus RTS

The well-known 24-bus RTS is used to apply the presented method. Parameters of the candidate lines are listed in Table 4, while resistances of lines are assumed to be one fifth of their corresponding reactances. Detailed data and topology of the RTS can be found in [25]. In order to put the transmission lines under more stress, active power demands and maximum active power generation capacities are multiplied by 2 for each generator. A 32-sided regular polygon is used to model the circle (see Appendix for more details).

The parameter σ was set to be 25×8760. The execution time was 3.32 seconds. Simulations show for the LAC-OPF that lines 8, 10 and 11 should be built within the planning horizon. Generating units 2, 10, 11, 14, 19, 20, 31 and 32 will produce active powers of 29.4 MW, 145.5 MW, 0 MW, 12.7 MW, 15.6, 0 MW, 216.9 MW and 0 MW, respectively; other units will operate at their maximum capacities. Table 5 indicates the results for various σ, showing considerable changes in results when σ varies. Using a DC-TEP approach for this case shows that lines 8 and 10 are constructed. This can be justified as reactive power is neglected in the DC approach, and therefore more transmission line capacities are available; resulting in lower required investment cost. Also, in an AC-TEP approach the candidate lines 5, 8, 9 and 10 are selected to be built which explicitly shows that the obtained solution is sub-optimal due to the non-convexity nature of the AC-OPF equations.

3.4. Fourth case study: Iran 400-kV simplified network

As the last test, a realistic power system is chosen; i.e., Iranian 400-kV power system. The topology and data of the network can be found in [11]. Power factor of loads is set to be 0.9 as a typical value. Instead of considering a single period as in previous case studies, a dynamic approach is selected for this case. To do so, an interest rate of 8% is regarded. Impedances of three-bundled and two-bundled 400-kV overhead lines are considered to be $0.0192 + j0.288\ \Omega$/km and $0.0288 + j0.3296\ \Omega$/km, respectively. Also, annual load growth is considered to be equal to 5% in average. The system is comprised of 52 buses, 28 generating units and 27 candidate lines. A planning horizon of 16 years is considered which is divided into two sub-periods.

The problem was run for different values of n. Simulations have been reported in Table 6. As it can be seen from the obtained results, the consumed times to reach the optimal solution will increase significantly by increasing the number n. To reduce the solution time, the number n can be different for various lines. It clearly depends on the operating point of active and reactive power for each line in the corresponding P–Q plane. The number n have to be big for highly congested and heavily loaded lines; but, n can be small without losing any generality for the lines operating far from their limits. Solving the TEP using simple DC power flow might be helpful to identify the most congested lines or areas. In the meanwhile,

[1] Please note that 8760 is the number of hours per year.
[2] It is to be noted that to calculate LMPs, the objective function has been modified to include only the generation offers (or equivalently operating cost) i.e. investment cost must be removed from the aforementioned objective function.

Table 6
Results from different cases for Iran 400-kV power system.

	Number of single equations/continuous variables/discrete variables	Elapsed time (min)
$M=10$ $n=8$	3,910,760/1,828,279/54	3.38
$M=10$ $n=16$	5,122,152/1,828,279/54	3.72
$M=10$ $n=32$	7,544,936/1,828,279/54	6.43
$M=10$ $n=64$	12,390,504/1,828,279/54	43.14

Table 7
Optimal solutions for Iran 400-kV power system.

	Candidate lines to be built
Sub-period 1	1–49, 4–50, 7–10, 7–23, 7–24, 24–29, 49–50, 23–32
Sub-period 2	4–50, 7–10, 7–12, 7–24, 10–12, 13–14, 18–19, 39–40, 42–43

selecting the number n would become more effective by experience. The same candidate lines are selected to be built for $n=32$ and $n=64$, while the results will be different for smaller value of n which verify that the quality of the methodology depends upon the number n. Table 7 shows that which candidate lines should be added to the power system during each sub-period. As it can be seen from the table, the most lines connected to bus 7 are needed to be reinforced or constructed because the main electricity demand is located at bus 7. Also it is to be noted that these lines are highly congested and therefore one should care about selecting the number n for these lines. In addition, an integrated framework for simultaneous reactive power planning and transmission expansion planning is suggested. This might lead to more optimal plan in power system and less power losses. Moreover, the uncertainty related to the generation capacity expansion planning and its effect on TEP have to be addressed precisely for such a real large-scale power network.

4. Conclusion

In this paper a new expansion planning model was formulated and applied to several power systems. The presented method uses the AC-OPF for solving the TEP problem in order to get a more accurate and real picture of both active and reactive power flow in the network. The AC-OPF–based TEP is an MINLP that is transformed into an MILP by the proposed method. A new linearization method is presented to transform the nonlinear AC model to a linear one. The formulated problem then can be solved by the available commercial MILP software. Moreover, due to the linearity of the proposed formulated problem, the global optimal solution is guaranteed to be found by many existing algorithms and software which are reliable and efficient.

The main difficulties and disadvantages of the presented methodology are to deal with the dimensionality and the mathematical computation burden of the problem, in particular when the size of the power system gets larger. This requires sufficient memory and high-speed processors to solve the MIP problem. With increasing system size, the execution time of the problem will increase as well. However, this depends considerably on the number of binary variables rather than the number of blocks or segment used in piecewise linearization approach. As a solution for this case, in order to reduce the search space the method can be applied to the high-voltage transmission lines initially, and then the planning can be conducted for lower voltage level transmission lines.

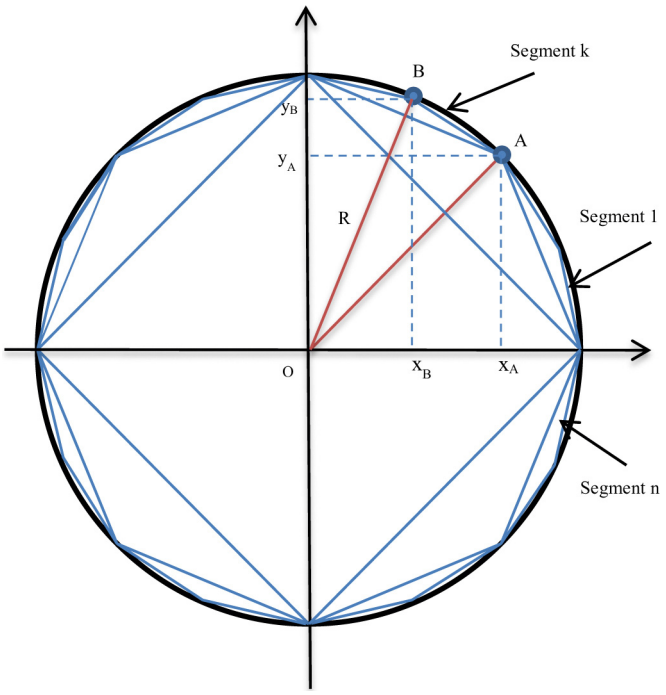

Fig. A1. A circle with radius R.

Appendix.

This appendix describes a simple proof of transformation of the nonlinear equation in the form of $x^2+y^2 \le R^2$ (a circle with radius R in the Cartesian coordinates) into n linear equations like (A2). Consider a circle with radius R as shown in Fig. A1. This circumscribed circle[3] or circum circle can be estimated by a n-sided convex regular polygon.

The line equation that directly connects point A to point B can be written as below:

$$y - R\times\sin\left(\frac{360^\circ k}{n}\right) = \frac{\sin(360^\circ k/n)-\sin(360^\circ/n(k-1))}{\cos(360^\circ k/n)-\cos(360^\circ/n(k-1))}\left(x - R\times\cos\left(\frac{360^\circ k}{n}\right)\right) \quad \text{(A1)}$$

Manipulating Eq. (A1) will lead to the following equation:

$$\left(\sin\left(\frac{360^\circ k}{n}\right)-\sin\left(\frac{360^\circ}{n}(k-1)\right)\right)x-\left(\cos\left(\frac{360^\circ k}{n}\right)-\cos\left(\frac{360^\circ}{n}(k-1)\right)\right)y-R\times\sin\left(\frac{360^\circ}{n}\right)=0 \quad \text{(A2)}$$

In a simple format assuming $\alpha=360^\circ k/n$ and $\beta=360^\circ k/n(k-1)$ we will obtain:

$$(\sin\ \alpha-\sin\ \beta)x-(\cos\ \alpha-\cos\ \beta)y-R\times\sin(\alpha-\beta)=0 \quad \text{(A3)}$$

The higher the number of segments is used to model the circle the more accurate results will be obtained but at the expense of more computational time.

References

[1] J. Choi, T.D. Mount, R.J. Thomas, Transmission expansion planning using contingency criteria, IEEE Trans. Power Syst. 22 (4) (2007) 2249–2261.

[3] It is assumed the circle is circumscribed to the regular polygon. One may assume that the circle is inscribed to the regular polygon.

[2] C.W. Lee, K.K. Ng, J. Zhong, F. Wu, Transmission expansion planning from past to future, Public Saf. Commun. Eur. (2006) 257–265.
[3] G. Latorre, R. Cruz, J.M. Areiza, A. Villegas, Classification of publications and models on transmission expansion planning, IEEE Trans. Power Syst. 18 (2) (2003) 938–946.
[4] N. Alguacil, A.L. Motto, A.J. Conejo, Transmission expansion planning: a mixed-integer LP approach, IEEE Trans. Power Syst. 18 (3) (2003) 1070–1077.
[5] M.C. Da Rocha, J.T. Saraiva, A multiyear dynamic transmission expansion planning model using a discrete based EPSO approach, Electr. Power Syst. Res. 93 (2012) 83–92.
[6] J.A. Aguado, S. Torre, J. Contreras, A.J. Conejo, A. Martinez, Market-driven dynamic transmission expansion planning, Electric Power Syst. Res. 82 (1) (2012) 88–94.
[7] B. Graeber, Generation and transmission expansion planning in southern Africa, IEEE Trans. Power Syst. 2 (1999) 983–988.
[8] M. Kandil, S. El-Debeiki, N. Hasanien, Rule-based system for determining unit locations of a developed generation expansion plan for transmission planning, IEE Proc. Gener. Transm. Distrib. 147 (1) (2000) 62–68.
[9] A. Khodaei, M. Shahidehpor, S. Kamalnoa, Transmission switching in expansion planning, IEEE Trans. Power Syst. 25 (3) (2010) 1722–1733.
[10] V.S.K.M. Balijepalli, S.A. Khaparde, A Holistic approach for transmission system expansion planning studies: an Indian experience, IEEE Trans. Power Syst. 5 (2) (2010) 199–212.
[11] P. Maghouli, S. Hosseini, M. Oloomi, M. Shahidehpour, A scenario-based multi-objective model for multi-stage transmission expansion planning, IEEE Trans. Power Syst. 26 (1) (2011) 470–478.
[12] P. Maghouli, S. Hosseini, M. Oloomi, M. Shahidehpour, A multi-objective framework for transmission expansion planning in deregulated environments, IEEE Trans. Power Syst. 24 (2) (2009) 1051–1061.
[13] Q. Zhou, L. Tesfatsion, C. Liu, R. Chu, W. Sun, Nash approach to planning merchant transmission for renewable resource integration, IEEE Trans. Power Syst. 28 (3) (2012) 2086–2100.
[14] A.M. Leite da Silva, L. Manso, W. Sales, S.A. Flávio, G.J. Anders, Chronological power flow for planning transmission systems considering intermittent sources, IEEE Trans. Power Syst. 27 (4) (2012) 1722–1733.
[15] Y. Gu, J.D. McCalley, M. Ni, Coordinating large-scale wind integration and transmission planning, IEEE Trans. Sustain. Energy 3 (4) (2012) 652–659.
[16] T. Akbari, A. Rahimikian, A. Kazemi, A multi-stage stochastic transmission expansion planning method, Energy Convers. Manage. 52 (2011) 2844–2853.
[17] T. Akbari, S. Zolfaghari, A. Kazemi, Multi-stage stochastic transmission expansion planning under load uncertainty using benders decomposition, Int. Rev. Electr. Eng. 4 (2009) 976–984.
[18] M.J. Rider, A.V. Garcia, R. Romero, Power system transmission network expansion planning using AC model, IET Generation, Transm. Distrib. 1 (5) (2007) 731–742.
[19] M. Rahmani, M. Rashidinejad, E.M. Carreno, R. Romero, Efficient method for AC transmission network expansion planning, Electr. Power Syst. Res. 20 (9) (2010) 1056–1064.
[20] R.A. Jabr, Polyhedral formulations and loop elimination constraints for distribution network expansion planning, IEEE Trans. Power Syst. 28 (2) (2013) 1888–1897.
[21] T. Akbari, A. Rahimikian, M. Tavakoli Bina, Security-constrained transmission expansion planning: a stochastic multi-objective approach, Electr. Power Energy Syst. (IJEPES) 43 (1) (2012) 444–453.
[22] El.I Samahy, K. Bhattacharya, C. Cañizares, M.F. Anjos, J. Pan, A procurement market model for reactive power services considering system security, IEEE Trans. Power Syst. 23 (1) (2008) 137–149.
[23] D.P. Bertsekas, Nonlinear Programming, Athena Scientific, NH, 1999.
[24] Generalized Algebraic Modeling Systems (GAMS), 2013, Available from: http://www.gams.com
[25] IEEE Committee Report, The IEEE reliability test system – 1996, IEEE Trans. Power Syst. 14 (3) (1999) 1010–1020.